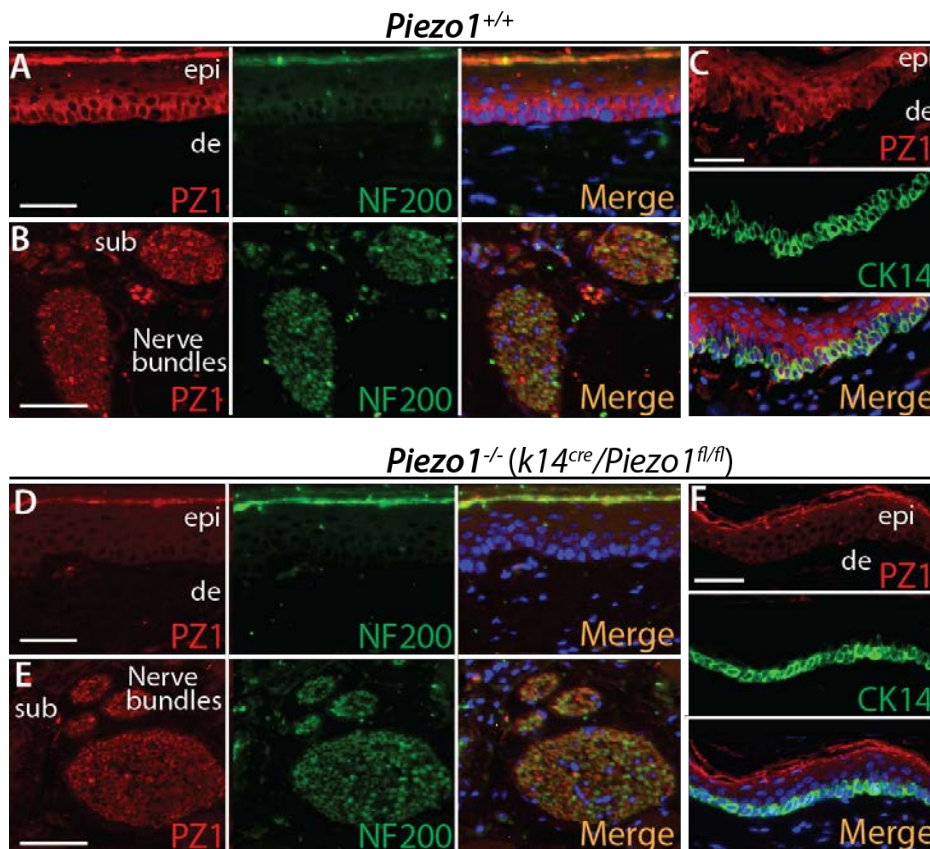


## Supplemental Figures

### Title: Piezo2 mechanosensitive ion channel is located to sensory neurons and non-neuronal cells in rat peripheral sensory pathway: implications in pain

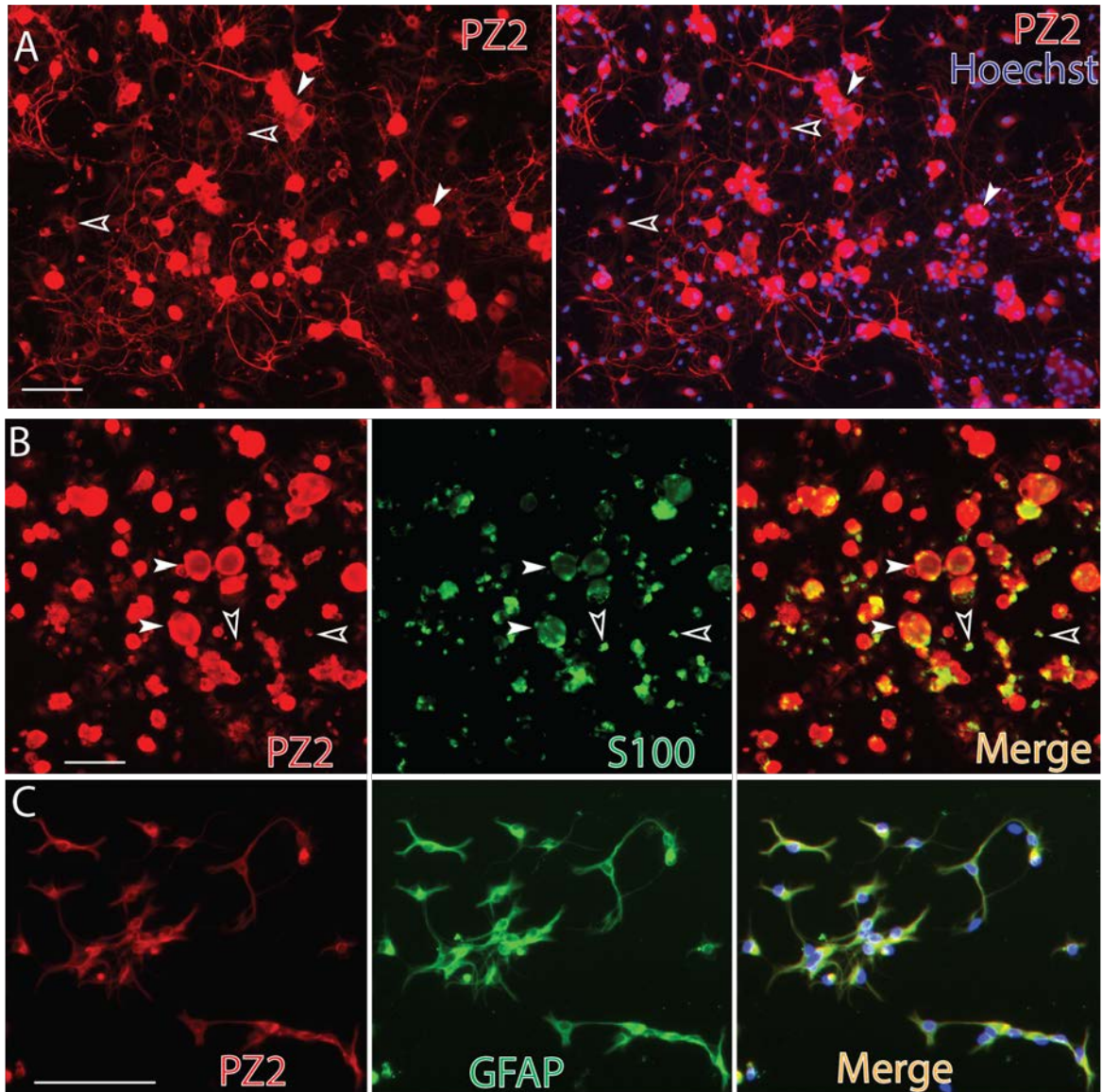
Seung Min Shin<sup>1</sup>, Francie Moehring<sup>2</sup>, Brandon Itson-Zoske<sup>1</sup>, Fan Fan<sup>3</sup>, Cheryl L. Stucky<sup>2</sup>, Quinn H. Hogan<sup>1,4</sup>, and Hongwei Yu<sup>1,4\*</sup>

<sup>1</sup> Department of Anesthesiology, <sup>2</sup> Department of Cell Biology, Neurobiology and Anatomy, Medical College of Wisconsin, Milwaukee, WI 53226. <sup>3</sup> Department of Pharmacology and Toxicology, Mississippi University Medical Center, Jackson, Mississippi 39216. <sup>4</sup> Zablocki Veterans Affairs Medical Center, Milwaukee, Wisconsin 53295



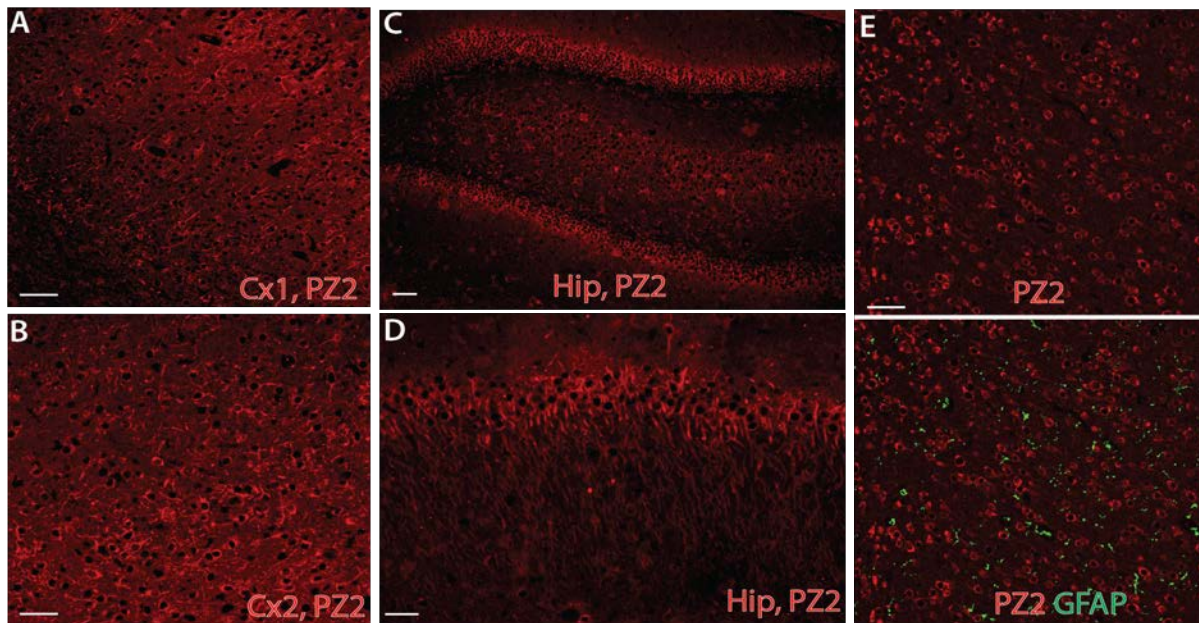
#### Suppl. Fig. 1. IHC validation of 1 Piezo1 antibody in K14cre/Piezo1fl/fl mice

Representative IHC montage images of colabeling of Piezo1 (PZ1, red), including NF200 and CK14 on FFPE sections of hindpaw skin from wide-type (WT) mice (A-C) and Piezo1-ko mice (C-D). Scale bar: 50m for all. Epi., de., and sub. denote epidermic, dermis, and subcutaneous, respectively. The keratinocyte Piezo1-IR signals in WT mice was dramatically decreased in Piezo1-ko mice (*cf.* A and C of WT to D and F of Piezo1-ko, respectively), while no notable change of Piezo1-IR signals detected in subcutaneous nerve bundles between WT and Piezo1-ko mice.



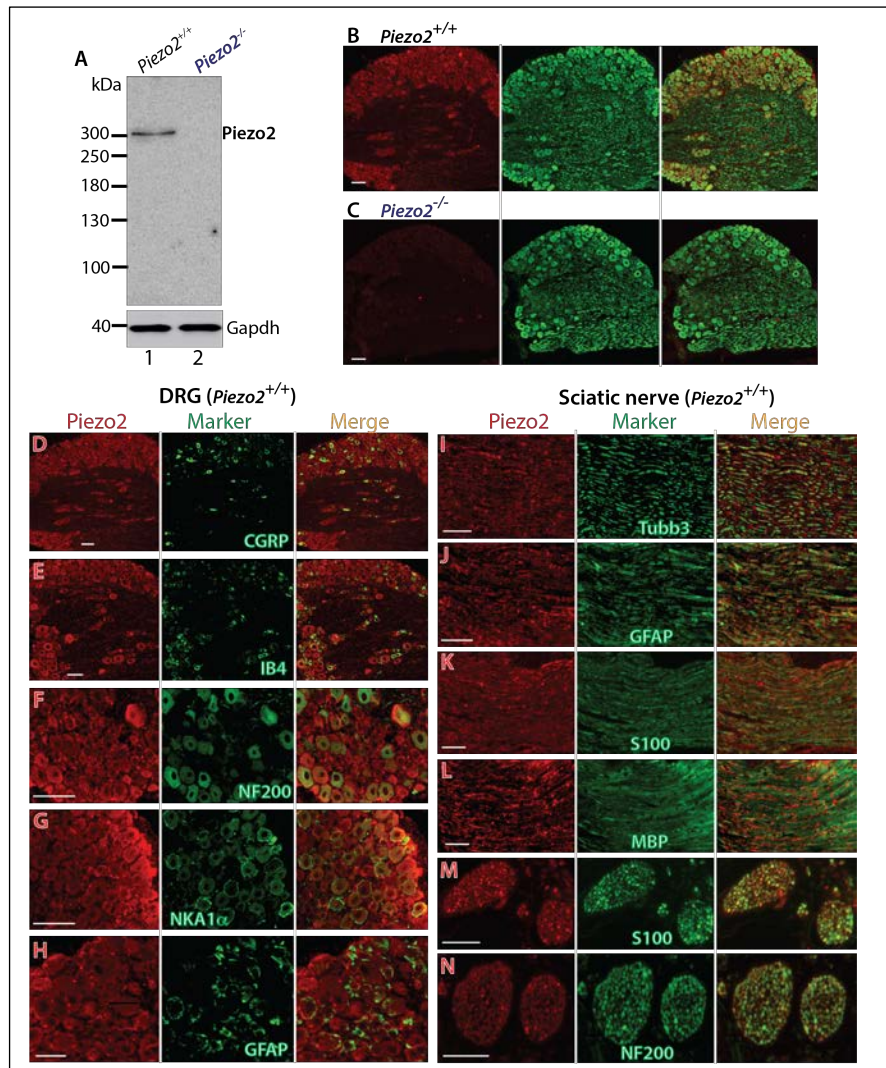
**Suppl. Fig. 2. ICC of Piezo2 (PZ2) in DRG dissociated culture.**

Representative montage images of Piezo2 immunostaining by ICC on DRG dissociated culture at Days In Vitro (DIV)=1 show immunoreactivity of Piezo2 (red) in neuronal somata and their axons (white arrowheads), as well as smaller glia-like cells and their neurites (empty arrowheads) (A). Representative montage images of ICC double immunostaining on DRG dissociated culture (DIV=0.25) show Piezo2 (red, white arrowheads) immunopositivity in all-sized neurons and co-stained with S100-positive (green, empty arrowheads) glia cells (B). Representative montage images of ICC double immunostaining on DRG dissociated culture (DIV=2) show immunocolocalization of Piezo2 (red) with GFAP-positive (green) glia cells (C). Scale bars: 100  $\mu$ m for all.



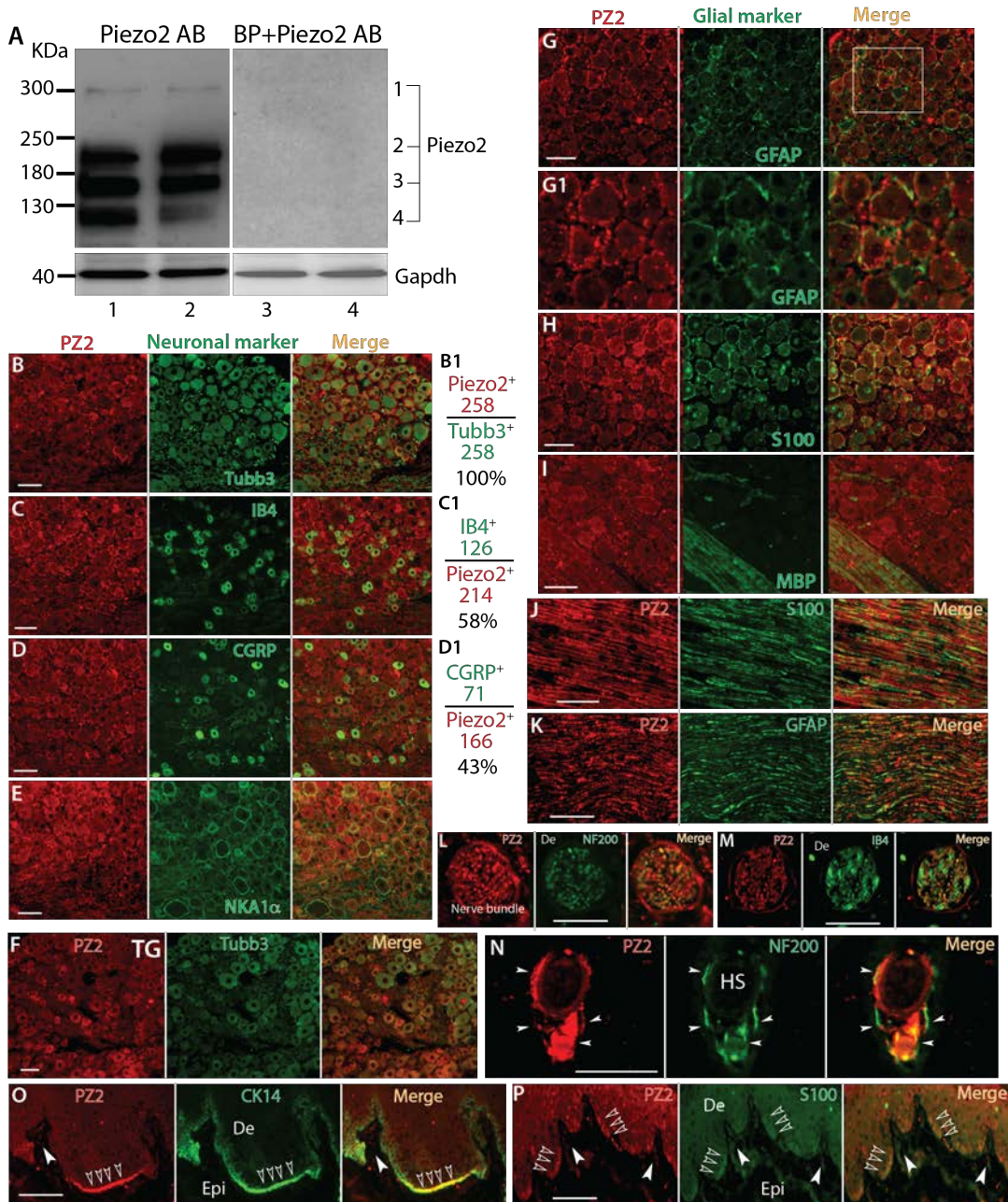
**Suppl. Fig. 3. IHC detection of Piezo2 expression in brain neurons.**

Representative IHC images show detection of Piezo2 (PZ2) expression (red) in the neurons of prefrontal cerebral cortex (Cx1) (A), lateral cerebral cortex (Cx2) (B), and hippocampus (Hip) (C, D) areas of brain FFPE sections from naïve adult rat. Representative montage images (vertical) show absence of PZ2 (red) in the GFAP-positive astrocytes (green) in naïve rat brain (E). Scale bars: 25  $\mu$ m for all.



**Suppl. Fig. 4. Validation of a different Piezo2 antibody in detection of Piezo2 (PZ2) expression.**

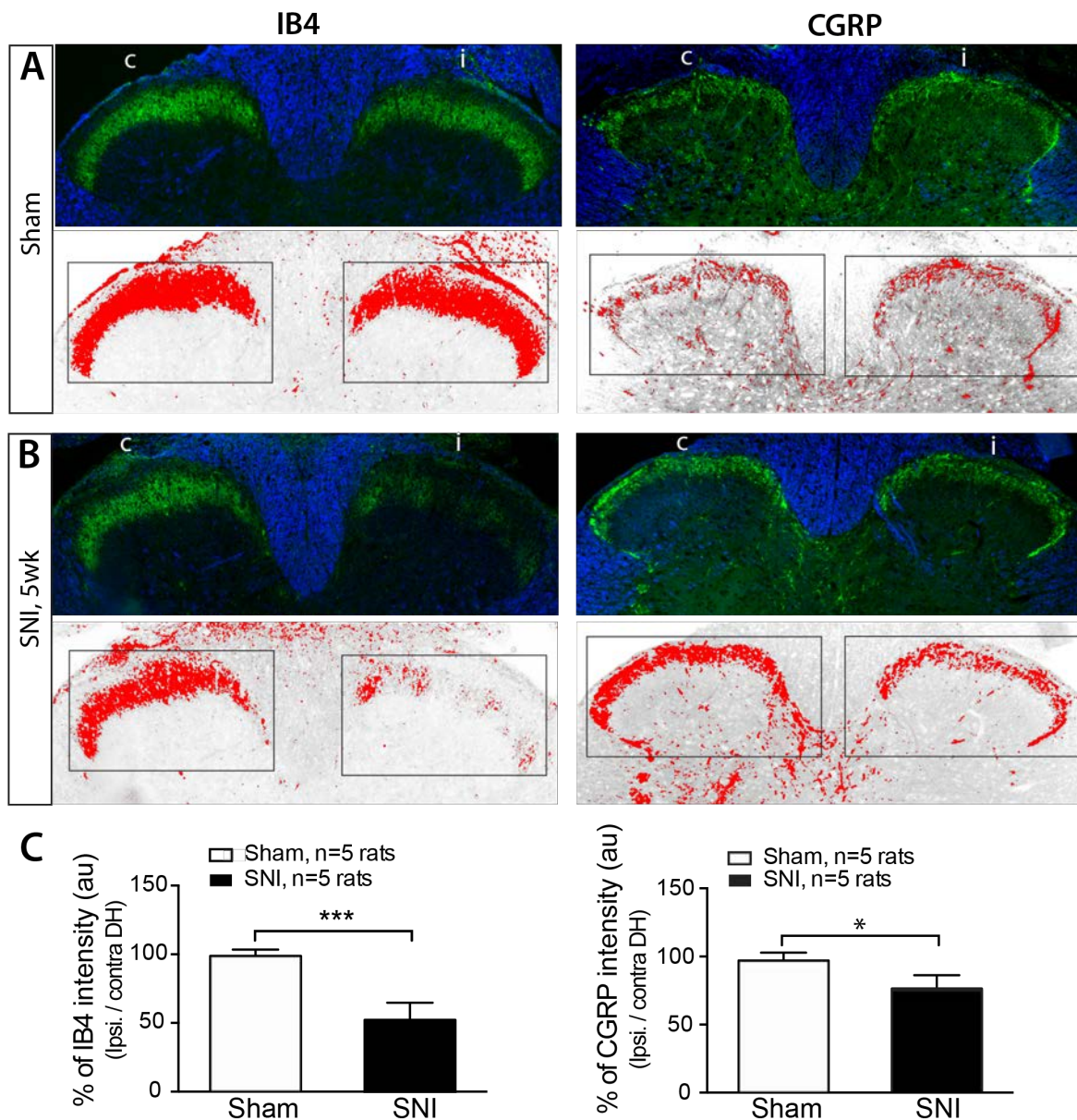
In DRG from wild-type (wt) mouse, Piezo2 antibody (Alomone) detected a strong single ~300kDa band by IB (A) and Tubb3 labeled pan-PSN expression profile (B), whereas Piezo2 IB and IHC signals were disappeared in the DRG from Piezo2-ko mouse (*Hoxb8cre/Piezo2<sup>fl/fl</sup>*) (A, C). Representative montage images of double immunostaining (double-IS) on DRG sections from wt mice revealed Piezo2-IR (red) and a selection of markers (green), including CGRP (D), IB4 (E), NF200 (F), NKA1 $\alpha$  (G), and GFAP (H) showing immunocolocalization (yellow) in merged images. Representative montage images of double-IS on sciatic nerve sections from wt mice revealed Piezo2-IR (red) and a selection of markers (green), including Tubb3 (I), GFAP (J), S100 (K), and MBP (L). Representative montage images displayed Piezo2-IR (red), S100 (M, green) and NF200 (N, green), showing colocalization in merged images (yellow) in nerve bundles of dermis sections. Scale bars: 50  $\mu$ m for all.



**Suppl. Fig. 5. Characterization of a different Piezo2 antibody in detection of Piezo2 (PZ2) expression.**

In DRG lysate, Piezo2 antibody (Alomone) detects several bands at approximate 310, 240, 180, and 130 kDa and marked as putative “isoforms” 1-4 of the target protein, since they are eliminated by preincubation with excess immunogenic peptide (A). Representative montage images of double immunostaining (double-IS) on DRG sections reveal Piezo2-IR (red) and a selection of neuronal markers (green), including Tubb3 (B), IB4 (C), CGRP (D), and NKA1 $\alpha$  (E), showing immunocolocalization (yellow) in merged images. Representative montage images of double-IS

on trigeminal ganglia (TG) section reveal Piezo2-IR (red) and Tubb3 (green) (**F**). The panels in the right-side of **B-D** are the percentage of Piezo2-IR neurons overlaid to Tubb3-positive neurons (**B1**), as well as IB4- (**C1**) and CGRP-positive neurons (**D1**) overlaid to Piezo2-IR neurons and the numbers are the counted Piezo2-IR neurons (red) and marker-IR neurons (green) in double labeling sections. Representative montage images of double-IS on DRG sections display Piezo2-IR (red) and a selection of glial cell markers (green), including GFAP (**G**) with the region within the square shown at high magnification (**G1**), S100 (**H**), MBP (**I**), showing immunocolocalization (yellow) in merged images. Representative montage images of double-IS on sciatic nerve sections reveal Piezo2-IR (red) and S100 (**J**) and GFAP (**K**), showing immunocolocalization (yellow) in merged images. Representative montage images of double-IS on the hindpaw skin display Piezo2-IR (red), NF200 (green) (**L**) and IB4 (green) (**M**), NF200 (green) (**N**, Lanceolate endings pointed by by white arrowheads), CK14 (green) (**O**, epidermal Merkel cells pointed by empty arrowheads and Meissner's corpuscles pointed by white arrowheads. HF: hair follicle), S100 (**P**, epidermal melanocytes pointed by empty arrowheads and Meissner's corpuscles pointed by white arrowheads), showing immunocolocalization (yellow) in merged images. Scale bars: 50  $\mu\text{m}$  for all.



**Suppl. Fig. 6. Validation of the methods to quantify DH immunostaining intensity.**

IB4 and CGRP immunolabeled fluorescent intensities in spinal DH of sham control (A, top) and SNI (B, top) were inverted; the upper and lower threshold optical intensities of IB4 and CGRP signals adjusted to encompass and match the IR that appears in red (A, B, bottom), respectively; and quantified as described in Method. The rectangles (A, B, bottom) positioned over laminae territory throughout the mediolateral axis on the contralateral and ipsilateral DHs. Scale bars: 100  $\mu\text{m}$  for all. The integrated density (product of area and density) calculated by use of ImageJ, and fold change (ratio of ipsilateral/contralateral) summarized in the bar charts (C). \* and \*\*\* denotes  $p < 0.05$  and  $p < 0.001$  by two-tailed unpaired Student's *t*-test. c, contralateral and i, ipsilateral.